ChemComm

ROYAL SOCIETY OF CHEMISTRY

COMMUNICATION

View Article Online
View Journal | View Issue





Cite this: *Chem. Commun.*, 2020, **56**, 1286

Received 7th October 2019,
Accepted 21st December 2019

DOI: 10.1039/c9cc07851g

rsc.li/chemcomm

# *In situ* formation and solid-state oxidation of a triselenane NSeN-pincer MOF†

Shichao He, Laynee L. Allemond, Samuel G. Dunning, Joseph E. Reynolds III, Vincent M. Lynch and Simon M. Humphrey *

**Controlled partial decomposition of 2-selenonicotinic acid in the presence of $Co^{2+}$ or $Ni^{2+}$ resulted in the *in situ* formation of an unusual MOF based on triselenane ligands (RSeSeSeR) coordinated to $M^{2+}$ centers as NSeN-pincers. Post-synthetic oxidation by treatment with aqueous $H_2O_2$ facilitates its solid-state conversion into a $RSeO_2^-$ molecular coordination complex, which was tracked *via* powder X-ray diffraction studies and by single-crystal structural resolution of the final product.**

The discovery of new metal–organic frameworks (MOFs) continues to rely predominantly on the use of organic components with hard donor groups (*e.g.*, carboxylates, azolates) *via* solution-phase assembly with high-valent metal ions.[1] MOFs based on softer, more covalent metal–ligand bonds between low-valent metals and diffuse organic donors remain rare.[2] Access to such MOFs could improve intra-framework electronic conductivity,[3] magnetic superexchange,[4] and would enable the incorporation of lower-valent metal ions of relevance to catalysis.[5,6]

MOF assembly based exclusively on soft coordination bonds[7] (*e.g.*, Figueroa's isocyanide MOFs[7a]) is synthetically challenging. One compromise involves the use of mixed-donor ligands, whereby hard donor groups facilitate the formation of stable MOF architectures, while also enabling the incorporation of softer functionalities.[8] We recently demonstrated the preparation of an organoarsine MOF using tris(*p*-carboxylato)triphenylarsine ligands.[9] Coordination to hard Co(II) inorganic clusters provided a porous MOF decorated with abundant $R_3As$ sites that were able to coordinate Au(I)Cl in the solid state; retention of crystallinity permitted full structural resolution.[9] In terms of solid-state magnetism, MOFs containing magnetic networks bridged with more diffuse donor atoms (*e.g.*, $NCS^-$,[10] $RS^-$[11]) have been shown to engender stronger magnetic ordering, leading to higher $T_C$ values.[10,11] We previously employed *n*-mercaptonicotinic acid (*n*-mna, $C_6H_3N$-*n*-SH-3-$CO_2H$; $n$ = 2, 6) to prepare magnetic MOFs with S-bridged 3D magnetic lattices; an example containing $[–Co–S–Co–S–]_\infty$ bridges had a $T_C$ = 68 K.[11a]

Examples of MOFs containing low-valent Se formally coordinated to metal ions remain rare and are mostly limited to low-dimensional coordination polymers based on neutral selenoethers.[12] Following our previous studies using *n*-mna, we prepared 2-selenonicotinic acid (2-Sena; $C_5H_3N$-2-SeH-3-$CO_2H$; Scheme 1) with the intention of using this ligand to synthesize isostructural materials containing more highly diffuse M–Se–M linkages. Our initial work has instead generated a series of unique and unexpected synthetic results due to the apparent non-innocence of 2-Sena as a MOF precursor.

A convenient route for the gram-scale synthesis of 2-Sena is summarized in Scheme 1. Treatment of 2-chloronicotinic acid (**1**) with Se metal, Na metal and $NaBH_4$ in ethanol (to generate the putative species $Se_2^{2-}$)[13] gave the corresponding diselenide (**2**),[14] which was dissolved in basic water and reductively cleaved using hydrazine hydrate. The resulting sodium selenide salt was directly treated with HCl to give 2-Sena (**3**) as a yellow

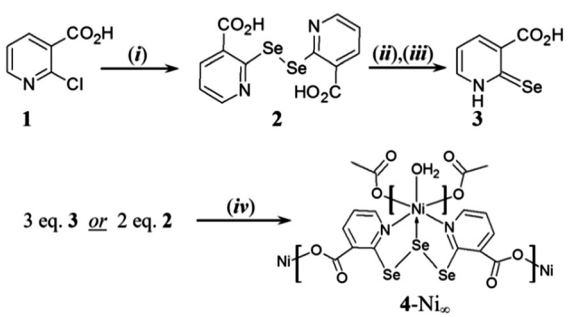


Scheme 1 Top: Synthesis of 2-selenonicotinic acid; (i) Se metal, Na metal, $NaBH_4$, ethanol, 0 → 70 °C, 4.5 h; (ii) $NaOH_{(aq)}$, $N_2H_4$, 60 °C, 4 h; (iii) conc. $HCl_{(aq)}$, 25 °C; (iv) $Ni(BF_4)_2$, DMF/$H_2O$ (1 : 2 v/v), 75 °C, 4 d.

*Department of Chemistry, The University of Texas at Austin, 100 East 24th Street, Stop A1590, Austin, Texas 78712, USA. E-mail: smh@cm.utexas.edu*

† Electronic supplementary information (ESI) available: Full experimental procedures for 2-Sena and SeCM-1; characterizing data for the ligands and SeCM-1: NMR, FT-IR, TGA, additional PXRD, and solid UV-vis data for 2-Sena, SeCM-1 and $[Ni(\mathbf{5})_2(OH_2)_2]$, respectively. CCDC 1909059–1909061. For ESI and crystallographic data in CIF or other electronic format see DOI: 10.1039/c9cc07851g

powder. Recrystallisation from hot water yielded **3** as mildly air-sensitive needles. Single crystal X-ray diffraction (SCXRD) revealed that the product was isolated as the pyridinium selone (Fig. S1, ESI†).

Next, we replicated a series of hydrothermal reactions in which **3** was employed in place of 2-mna to obtain selenolate-bridged analogues of previously reported thiolate-bridged magnetic MOFs.[11] Under the relatively harsh hydrothermal conditions employed in the original reactions (200 °C, pH > 10), ligand **3** decomposed to give crystalline (grey) Se, presumably because the C($sp^2$)–Se bond is more labile than the C–S bond in 2-mna.

By necessity, we next tried to form coordination polymers with **3** under more facile conditions, using mixed organic/aqueous solvent systems at lower temperatures. Reaction of **3** with $Ni(BF_4)_2$ in a 1 : 2 *N*,*N*-dimethylformamide (DMF)/$H_2O$ mixture at 75 °C resulted in the formation of green plate-like crystals in good yields. SCXRD revealed an unexpected product: the new material, hereafter referred to as SeCM-1 (SeCM = selenium coordination material), is a 2-D MOF that consists of unusual triselenane organic moieties (**4**; Scheme 1). SeCM-1 has the formula unit $[Ni(\mathbf{4})(OH_2)]_\infty$ and crystallizes into the tetragonal space group, $P4_2/ncm$ ($Z$ = 8; Fig. 1). Twice the asymmetric unit of SeCM-1 contains one complete Ni(**4**)($OH_2$) complex; Ni1, Se2 and O3 lie on a mirror plane (Fig. 1A). The central Se2 atom is formally coordinated to a Ni(II) ion (Ni1–Se2 = 2.455(2) Å) and the Se1–Se2–Se1A backbone has an angular arrangement (104.46(7)°) conforming to $sp^3$ hybridization. The aryl groups are arranged with the pyridyl-N donors (N1 & N1A; Fig. 1A) in a *cis* orientation. The triselenane ligand **4** thus adopts a facial NSeN-pincer embrace to Ni1; the coordination sphere of Ni1 is completed by two *syn*-coordinated carboxylates from neighbouring ligands (O2A & O2B) and a single terminal $OH_2$ ligand *trans* to Se2. The extended structure of SeCM-1 takes the form of a 2-D grid-like MOF with Ni(II) sites at the corners (Fig. 1B). Adjacent layers are closely packed in an eclipsed manner (Fig. 1C), providing 1-D channels parallel to the *c*-axis, with van der Waals accessible openings of 10.2 $Å^2$ (corner-to-corner; Fig. 1B).

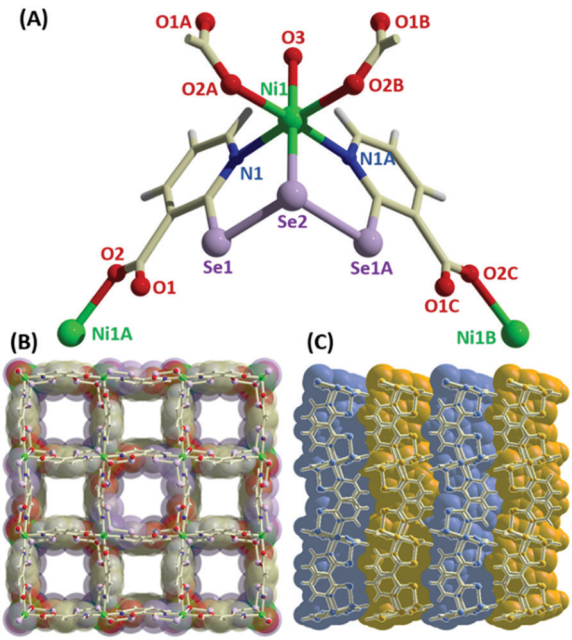


Fig. 1 (A) Twice the asymmetric unit of SeCM-1, showing triselenane ligand **4** coordinated to a single octahedral Ni1 in a *facial*-NSeN arrangement. (B) Space-filling rendering of the extended structure of SeCM-1 with superimposed ball-and-stick model, viewed in the crystallographic *ab*-plane. (C) Side view showing the close packing of 2D sheets; alternating sheets are drawn in yellow and blue.

The formation of SeCM-1 was apparently facilitated by Se extrusion, in which one equivalent of the selenol **3** was decomposed *in situ* to generate free Se and nicotinic acid. The Se was then inserted between $RSe^-$ fragments of two further equivalents of **3** to yield the triselenane, **4** ($\{C_5H_3N\text{-}2\text{-}Se\text{-}3\text{-}CO_2\}_2Se$), accompanied by coordination to Ni(II). There is scarce literature precedent for this type of reaction to form molecular triselenane complexes: it is known that $RSe^-$ reacts in solution with *n*Se to give the corresponding $RSe_n^-$ compounds.[14,15] A $R_2C{=}Se$-bearing N-heterocyclic carbene has also been used to prepare an $RSe_3R$ ligand,[16] but there are no previous examples of the direct formation of triselenane-functionalised materials by this method. Free organoselenanes are usually unstable due to labile Se redistribution.[16,17] To the best of our knowledge, there is only one other reported example of an isolable $RSe_3R$ complex, stabilized by direct coordination to Ru(II).[16] Here, *in situ* triselenane formation embedded within a MOF scaffold led to a crystalline material that is both air- and moisture-stable.

Further synthetic investigations revealed that an isostructural Co-based version of SeCM-1 could also be easily prepared using $CoCl_2$ as the metal precursor from a 2 : 3 : 3 v/v DMF/dioxane/$H_2O$ mixture (see ESI†). SeCM-1 could also be prepared in comparable yields using the diselenane intermediate **2** instead of the selenolate **3** (ESI†). In support of the premise that decomposition of **3** was responsible for the formation of **4**, heating of **3** in the absence of the M(II) precursors produced a red suspension of Se but no crystalline products. Furthermore, reactions using stoichiometric amounts of **3** in the presence of $Se{=}PPh_3$ as an extraneous source of Se resulted in formation of SeCM-1 with modestly improved yields.

Crystalline SeCM-1 is thermally stable up to 260 °C (thermogravimetric analysis, TGA; Fig. S2, ESI†). Both the Co and Ni analogues showed a defined 3.5% mass loss between 110–160 °C corresponding to the loss of a single coordinated $H_2O$ molecule per metal centre, in addition to 6.5% solvent loss from unbound solvates in the pores. The BET surface area of SeCM-1 was assessed using both $N_2$ and $CO_2$ (77 and 196 K, respectively), yielding values of 286 $m^2\ g^{-1}$ ($V_{pore}$ = 0.16 $cm^3\ g^{-1}$) and 392 $m^2\ g^{-1}$ ($V_{pore}$ = 0.20 $cm^3\ g^{-1}$). Studies using other probe gases revealed highly reversible Type-I adsorption–desorption behaviour for $N_2$, $CO_2$, $O_2$ (77 K), $H_2$ (77 K) and $CH_4$ (196 K), with capacities of 4.46, 4.87, 6.29, 7.81 and 2.77 mmol $g^{-1}$, respectively (Fig. 2). Notably, SeCM-1 showed the highest selectivity and capacity for $O_2$ sorption under standard cryogenic conditions, which is commonly not the case for MOFs because $O_2$ is less polarizable than gases such as $CO_2$.[18] The steep sorption of $O_2$ below $p/p_0$ = 0.05 (Fig. 2; red data) is indicative of an appreciable affinity towards $O_2$ physisorption and may be due to the abundant Se lone pairs that line the pore walls.

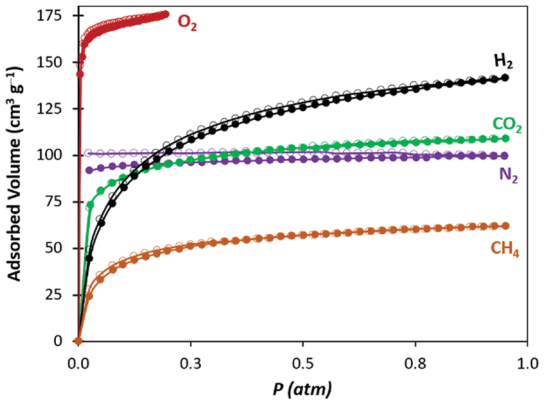


Fig. 2 Comparison of cryogenic adsorption–desorption isotherms obtained for various probe gases in Ni-SeCM-1.

Similarly, the $H_2$ sorption capacity in Ni-SeCM-1 is also unusually higher than either $CO_2$ or $N_2$.

Next, we attempted to exploit the immobilization of the elusive triselenane motif in SeCM-1 by controlled post-synthetic oxidation of the Se(II) centers. Gabbaï showed that a PTeP-pincer complexed to Au(I) could be partially oxidized using $H_2O_2$.[19] In our initial crude experiments, immersion of Ni-SeCM-1 crystals in aqueous $H_2O_2$ (3% w/w) resulted in the formation of a brick-red powder in addition to the crystals, which were unchanged (Fig. S3, ESI†). Upon standing, the red by-product slowly became bleached to a white amorphous powder (Fig. S4, ESI†). Decanting of the solution and amorphous solids resulted in the isolation of crystals that appeared to be morphologically unchanged.

SCXRD of a suitable single crystal revealed a new unit cell in a lower symmetry setting compared with SeCM-1. Full structural resolution revealed conversion to a new molecular complex that was solved in the triclinic space group $P\bar{1}$ ($Z = 1$) with formula $[Ni(\mathbf{5})_2(OH_2)_2]$ (Fig. 3). The new ligand **5** is a seleninic acid version of the original ligand, $(C_5H_3N\text{-}2\text{-}SeO_2\text{-}3\text{-}CO_2H)^-$. **5** was formed in the solid state by the re-extrusion of the central Se atom of the triselenane moiety in **4**, along with oxidation of the $RSe_2^-$ groups to give two $R(SeO_2)^-$ ligands.[20a] The molecular complex consists of a central octahedral Ni(II) centre that is coordinated by two chelating equivalents of **5** in a *trans* arrangement, with axially-coordinated $OH_2$ molecules.

This result is an unusual example of a solid-state transformation, induced by relatively harsh chemical oxidation, since the bulk transformation results in loss of the porous structure of the initial material; the estimated density change obtained from the SCXRD data is from 1.7 to 2.2 g $cm^{-3}$. The transformation could be achieved in as little as 10 min by treatment of SeCM-1 with 10% $H_2O_2$ (600 eq.), again resulting in highly crystalline product.

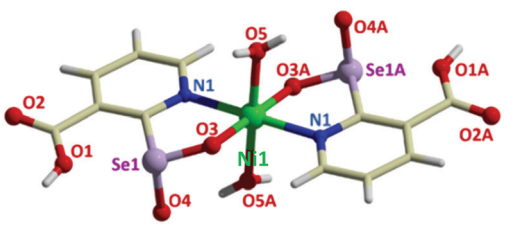


Fig. 3 Crystal structure of the molecular complex $[Ni(\mathbf{5})_2(OH_2)_2]$ formed by solid-state oxidation of Ni-SeCM-1.

In an effort to better understand the nature of this transformation, we used PXRD, FT-IR and *in situ* optical microscopy to track the process in bulk as a function of the relative $H_2O_2$ concentration; Fig. 4A–D and Fig. S5–S7 (ESI†) show the results of this study. The initial SeCM-1 crystallites are pale green blocks whose powder pattern is well-matched to the pattern simulated from the SCRXD data between 5–40° $2\theta$ (Fig. 4A and B, green data). Upon addition of one equivalent of $H_2O_2$ relative to **4** (*i.e.*, 1 eq. 'O' per $Se_3$ moiety) and allowing the crystals to stand overnight, the resulting PXRD pattern was unchanged (Fig. 4B, blue data). But, upon treatment with a further 9 eq. of $H_2O_2$ (*i.e.*, 10 eq. 'O' per $Se_3$), the PXRD pattern was markedly changed (Fig. 4A, red data). The sample still showed all of the reflections associated with SeCM-1 along with a significant number of new reflections. At this stage, the solid appeared to become red in colour. This visual effect was, in fact, caused by reflection of light from evolved particles of red Se. Gentle swirling released the Se, which subsequently floated on top of the $H_2O_2$ solution.

Finally, upon addition of a further 10 eq. of $H_2O_2$, the PXRD pattern matched with the simulated pattern expected for the molecular complex (Fig. 4A, yellow data) and no longer contained

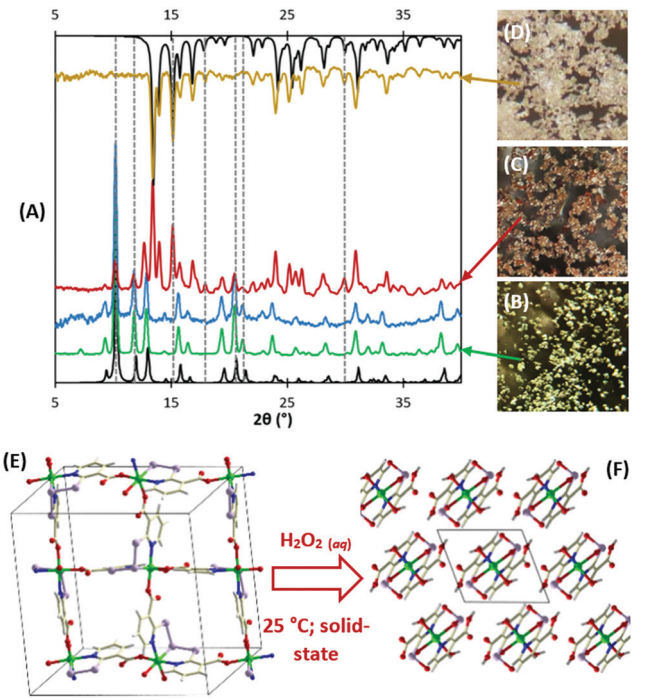


Fig. 4 (A) Comparison of PXRD patterns, bottom to top: SeCM-1 simulated data (black); as-synthesized Ni-SeCM-1 (green); 1 eq. $H_2O_2$ (blue); 10 eq. $H_2O_2$ (red); 20 eq. $H_2O_2$ (yellow); $[Ni(\mathbf{5})_2(OH_2)_2]$ simulated data (black). (B) Light microscope photograph of SeCM-1. (C) Photograph of intermediate with 10 eq. $H_2O_2$. (D) Photograph of the oxidized product. (E and F) Extended structures of SeCM-1 and $[Ni(\mathbf{5})_2(OH_2)_2]$, respectively, showing a comparative 3 × 3 arrangement of Ni centres.

reflections that could be exclusively indexed to the original SeCM-1 material. The resulting crystallites had the same size and morphology as the precursor SeCM-1, but were pale yellow in colour. Upon addition of excess $H_2O_2$ to drive the oxidation reaction to completion, the red Se was also gradually oxidized to white $SeO_2$.[21] Comparison of FT-IR spectra taken before and after oxidation (Fig. S6 and S7, ESI†) reveal new strong bands at 415 and 814 $cm^{-1}$, due to O–Se–O bending and Se=O stretching modes, respectively. A new broad band at 3262 $cm^{-1}$ for the H-bonded carboxylic acid was also observed.

The formation of the Ni(II) complex is in-line with the known reactivity of organoselenide-functionalized organic molecules with $H_2O_2$.[20] However, this result also provides a rare example of a deprotonated organoseleninic acid coordinated to a 3d metal ion. Consideration of the crystal structures of SeCM-1 (Fig. 4E) and the molecular product (Fig. 4F) offer some insights into the solid-state mechanism responsible for this unusual transformation. The distances between Ni centres and their spatial distribution do not alter to a significant degree in transition from one structure to the other. However, the ligand coordination geometry at each Ni(II) centre is markedly changed from *cis*-N donors in SeCM-1 (Fig. 4E) to *trans*-N donors in $[Ni(\mathbf{5})_2(OH_2)_2]$ (Fig. 4F). When viewed in the crystallographic orientations depicted, it can be understood how release of the central Se in SeCM-1 and cleavage of the Ni-OCO bonds would allow one ligand per Ni to 'hinge' up or down by 90°, resulting in the final *trans* orientation of ligands observed in $[Ni(\mathbf{5})_2(OH_2)_2]$. This process is accompanied by protonation of the carboxylate groups; since the reaction was conducted using aqueous $H_2O_2$, proton transfer would be favourable.

The initial results presented here using 2-Sena has revealed the potential to uncover new and unusual solid-state structures and behaviours, owing to the introduction of esoteric and chemically labile organic moieties into MOFs. Studies to further modify the triselenane pincer species in the solid-state for potential applications in catalysis are already under way.

This work was supported by the National Science Foundation under Grant No. DMR-1905701 and the Welch Foundation (F-1738). The authors thank Prof. E. Que, Dr I. Riddington and Dr Raluca Gearba for synthetic and analytical assistance and Prof. C. B. Mullins for his mentorship (S. H.).

## Conflicts of interest

There are no conflicts to declare.

## Notes and references

1 (*a*) D. A. Reed, B. K. Keitz, J. Oktawiec, J. A. Mason, T. Runčevski, D. J. Xiao, L. E. Darago, V. Crocellà, S. Bordiga and J. R. Long, *Nature*, 2017, **550**, 96–100; (*b*) H.-X. Deng, G. Sergio, K. E. Cordova, C. Valente, H. Furukawa, M. Hmadeh, F. Gándara, A. C. Whalley, Z. Liu, S. Asahina, H. Kazumori, M. O'Keeffe, O. Terasaki, J. F. Stoddart and O. M. Yaghi, *Science*, 2012, **336**, 1018–1023; (*c*) H.-C. Zhou, J. R. Long and O. M. Yaghi, *Chem. Rev.*, 2012, **112**, 673–674.

2 (*a*) Z. Z. Lu, R. Zhang, Y. Z. Li, Z. J. Guo and H. G. Zheng, *J. Am. Chem. Soc.*, 2011, **133**, 4172–4174; (*b*) K. Fan, S. S. Bao, W. X. Nie, C. H. Liao and L. M. Zheng, *Inorg. Chem.*, 2018, **57**, 1079–1089.

3 (*a*) X. Huang, P. Sheng, Z. Y. Tu, F. J. Zhang, J. H. Wang, H. Geng, Y. Zou, C. A. Di, Y. P. Yi, Y. M. Sun, W. Xu and D. B. Zhu, *Nat. Commun.*, 2015, **6**, 7408; (*b*) T. Kambe, R. Sakamoto, K. Hoshiko, K. J. Takada, M. Miyachi, J. H. Ryu, S. Sasaki, J. Kim, K. Nakazato, M. Takata and H. Nishihara, *J. Am. Chem. Soc.*, 2013, **135**, 2462–2465; (*c*) T. Pal, T. Kambe, T. Kusamoto, M. L. Foo, R. Matsuoka, R. Sakamoto and H. Nishihara, *ChemPlusChem*, 2015, **80**, 1255–1258.

4 (*a*) T. Neumann, M. Rams, Z. Tomkowicz, I. Jess and C. Näther, *Chem. Commun.*, 2019, **55**, 2652; (*b*) R. H. Dong, Z. T. Zhang, D. C. Tranca, S. Q. Zhou, M. C. Wang, P. Adler, Z. Q. Liao, F. Liu, Y. Sun, W. J. Shi, Z. Zhang, E. Zschech, S. C. B. Mannsfeld, C. Felser and X. L. Feng, *Nat. Commun.*, 2018, **9**, 2637.

5 (*a*) H. H. Fei and S. M. Cohen, *J. Am. Chem. Soc.*, 2015, **137**, 2191–2194; (*b*) S. G. Dunning, G. Nandra, A. D. Conn, W.-R. Chai, R. E. Sikma, J. S. Lee, P. Kunal, J. E. Reynolds III, J.-S. Chang, A. Steiner, G. Henkelman and S. M. Humphrey, *Angew. Chem., Int. Ed.*, 2018, **57**, 9295–9299; (*c*) A. M. Bohnsack, I. A. Ibarra, V. I. Bakhmutov, V. M. Lynch and S. M. Humphrey, *J. Am. Chem. Soc.*, 2013, **135**, 16038–16041.

6 (*a*) S.-S. Bao, G. K. H. Shimizu and L.-M. Zheng, *Coord. Chem. Rev.*, 2019, **378**, 577–594; (*b*) A. B. Redondo, F. L. Morel, M. Ranocchiari and J. A. V. Bokhoven, *ACS Catal.*, 2015, **5**, 7099–7103; (*c*) S. A. Burgess, A. Kassie, S. A. Baranowski, K. J. Fritzsching, K. Schmidt-Rohr, C. M. Brown and C. R. Wade, *J. Am. Chem. Soc.*, 2016, **138**, 1780–1783.

7 (*a*) D. W. Agnew, M. Gembicky, C. E. Moore, A. L. Rheingold and J. S. Figueroa, *J. Am. Chem. Soc.*, 2016, **138**, 15138–15141; (*b*) J.-H. Dou, L. Sun, Y.-C. Ge, W.-B. Li, C. H. Hendon, J. Li, S. Gul, J. Yano, E. A. Stach and M. Dinca, *J. Am. Chem. Soc.*, 2017, **139**, 13608–13611; (*c*) J. G. Park, M. L. Aubrey, J. Oktawiec, K. Chakarawet, L. E. Darago, F. Grandjean, G. J. Long and J. R. Long, *J. Am. Chem. Soc.*, 2018, **140**, 8526–8534.

8 (*a*) J.-P. He, N. W. Waggoner, S. G. Dunning, A. Steiner, V. M. Lynch and S. M. Humphrey, *Angew. Chem., Int. Ed.*, 2016, **55**, 12351–12355; (*b*) J. M. Falkowski, C. Wang, S. Liu and W.-B. Lin, *Angew. Chem., Int. Ed.*, 2011, **50**, 8674–8678.

9 R. E. Sikma, P. Kunal, S. G. Dunning, J. E. Reynolds III, J. S. Lee, J.-S. Chang and S. M. Humphrey, *J. Am. Chem. Soc.*, 2018, **140**, 9806–9809.

10 (*a*) C. Hua, J. A. DeGayner and T. D. Harris, *Inorg. Chem.*, 2019, **58**, 7044–7053; (*b*) J. Boeckmann, M. Wriedt and C. Näther, *Chem. – Eur. J.*, 2012, **18**, 5284–5289; (*c*) X.-R. Wu, H.-Y. Shi, R.-J. Wei, J. Li, L.-S. Zheng and J. Tao, *Inorg. Chem.*, 2015, **54**, 3773–3780.

11 (*a*) S. M. Humphrey, A. Alberola, C. J. G. García and P. T. Wood, *Chem. Commun.*, 2006, 1607–1609; (*b*) S. M. Humphrey, R. A. Mole, R. I. Thompson and P. T. Wood, *Inorg. Chem.*, 2010, **49**, 3441–3448; (*c*) S. M. Humphrey, R. A. Mole, M. McPartlin, E. J. L. McInnes and P. T. Wood, *Inorg. Chem.*, 2005, **44**, 5981–5983.

12 (*a*) C. A. Downes and S. C. Marinescu, *ACS Catal.*, 2017, **7**, 848–854; (*b*) W. Ji, J. Qu, S. Jing, D.-R. Zhu and W. Huang, *Dalton Trans.*, 2016, **45**, 1016–1024; (*c*) K. Malczewska-Jaskóła, W. Jankowski, B. Warżajtis, B. Jasiewicz, M. Hoffmann and U. Rychlewska, *Polyhedron*, 2015, **100**, 404–411.

13 (*a*) D. L. Klayman and T. S. Griffin, *J. Am. Chem. Soc.*, 1973, **95**, 197–199; (*b*) D. P. Thompson and P. Boudjouk, *J. Org. Chem.*, 1988, **53**, 2109–2112.

14 (*a*) L. Sancineto, A. Mariotti, L. Bagnoli, F. Marini, J. Desantis, N. Iraci, C. Santi, C. Pannecouque and O. Tabarrini, *J. Med. Chem.*, 2015, **58**, 9601–9604; (*b*) V. Nascimento, N. L. Ferreira, R. F. S. Canto, K. L. Schott, E. P. Waczuk, L. Sancineto, C. Santi, J. B. T. Rocha and A. L. Braga, *Eur. J. Med. Chem.*, 2014, **87**, 131–139.

15 A. Ahrika, J. Robert, M. Anouti and J. Paris, *New J. Chem.*, 2001, **25**, 741–746.

16 R. D. Dewhurst, A. R. Hansen, A. F. Hill and M. K. Smith, *Organometallics*, 2006, **25**, 5843–5846.

17 (*a*) T. M. Klapötke, B. Krumm, K. Polborn and M. Scherr, *Eur. J. Inorg. Chem.*, 2006, 2937–2941; (*b*) S. Kumar, K. Kandasamy, H. B. Singh, G. Wolmershahüser and R. J. Butcher, *Organometallics*, 2004, **23**, 4199–4208; (*c*) A. Ishii, S. Matsubayashi, T. Takahashi and J. Nakayama, *J. Org. Chem.*, 1999, **64**, 1084–1085.

18 (*a*) K. Sumida, D. L. Rogow, J. A. Mason, T. M. McDonald, E. D. Bloch, Z. R. Herm, T.-H. Bae and J. R. Long, *Chem. Rev.*, 2012, **112**, 724–781; (*b*) T. M. Tovar, I. Iordanov, D. F. S. Gallis and J. B. DeCoste, *Chem. – Eur. J.*, 2018, **24**, 1931–1937.

19 H.-F. Yang, T.-P. Lin and F. P. Gabbai, *Organometallics*, 2014, **33**, 4368–4373.

20 (*a*) G. Ribaudo, M. Bellanda, I. Menegazzo, L. P. Wolters, M. Bortoli, G. Ferrer-Sueta, G. Zagotto and L. Orian, *Chem. – Eur. J.*, 2017, **23**, 2405–2422; (*b*) H.-P. Xu, W. Cao and X. Zhang, *Acc. Chem. Res.*, 2013, **46**, 1647–1658.

21 C. Paulmier, *Selenium Reagents and Intermediates in Organic Synthesis*, Pergamon Press, 1986.